Photocatalytic Concrete Slab for Passive NOx Pollution Control

M.Palla, A. Vaddi, R. Asapu, D.Chen, K. Li, and R.Yuan, Photocatalysis & Green Composite Labs, Lamar University, Beaumont, Texas 77710

Extended Abstract

Introduction

NO$_x$ emissions have become a constraint for sustainable economic development due to ozone non-attainment [1-5]. Under light illumination over a photocatalyst free radicals are generated to oxidize or decompose pollutants. While volatile organic compounds (VOCs) are oxidized to water, CO_2, and chloride, NOx are oxidized to nitric acid, neutralized by the alkaline materials in concrete, and washed away by rain [6-9]. Ozone can be decomposed to oxygen over photocatalysts. Recent developments in Europe Japan, Hong Kong, and US have demonstrated the interest in deploying photocatalytic technologies for environmental remediation. The photocatalytic coating has potential to economically reduce nitrogen oxides (NOx) emissions at ambient conditions nearly maintenance-free [10-12].

We report here the application of photocatalytic coatings on a concrete slab to simulate road pavements for passive NOx pollution control. Catalysts tested include Degussa P-25 TiO$_2$ and TiO$_2$ - boosted with BaTiO$_3$, Nd$_2$O$_3$, and Fe$_2$O$_3$ [13-16]. Both NO and NO$_2$ oxidation including the effects of inlet NO concentration, residence time, and humidity are investigated. The removal efficiencies are in the range of 86-93% from 200 ppb-2000 ppb NO. Relative Humidity (RH) is seen to have some beneficial effect at <35% RH while lowering NO conversion by ~10% at > 35% RH. The additives Nd$_2$O$_3$, Fe$_2$O$_3$, and BaTiO$_3$ are observed to depress the NO$_2$ generation while improving NO conversion when using fiber-optic as a support. When tested on catalytic concrete slabs, however, Degussa P-25 offers the best NO removal, even though Fe2O3 and Nd2O3 offer better NO2 suppression. The optimal TiO2 to cement ratio is of interest because TiO2:SiO2 photocatalyst shows twin peaks in their activity in atrazine oxidation and the fact that cement also contains Fe2O3. A CFD simulation of NOx plumes from a tail pipe shows the likely distribution of concentration and residence time due to dispersion; that, in turn, can provide a useful guide for future lab investigations.

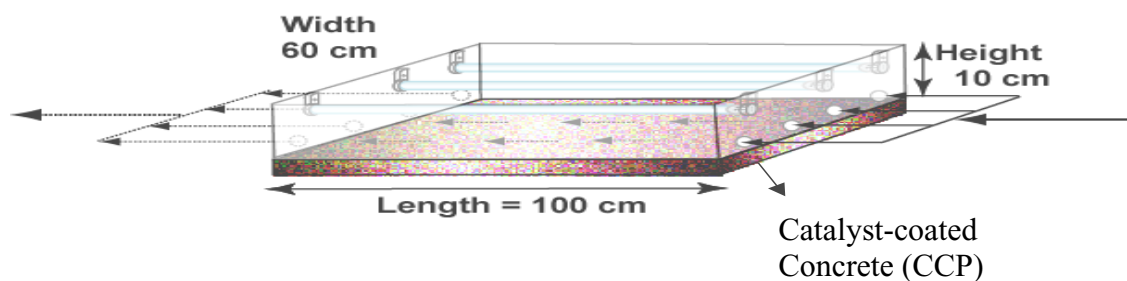Experimental Setup - Catalyst-Coated Concrete Photoreactor (CCP)

Figure 1 (a) Detailing of Concrete Slab and Wooden Mold

The catalyst-coated Concrete Photoreactor (CCP) is shown in Figure 1 (a)-(c). Three 50W (800 mA) fluorescent lamps (Philips, Model # F36T12/D/HO) are used with a total radiation of 250 W/m^2 as compared to a high-noon solar radiation of 1.44 Langleys/min (1004.18 W/m^2). The Teledyne API NOx ambient level/trace level analyzer (Model # 200EU 20B-41) is used for NOx sampling.

Figure 1 (b)   Lamp Fixture Assembly   *Figure 1(c)*   Simulated Solar Radiation

The operating conditions of the NO oxidation over a catalytic cement surface are given below: Residence Time: 20 min; Light Source: 50W Fluorescent Light ; Reactant: NO (inlet concentration 2.5 ppm); Catalyst on Concrete Surface: TiO2 Degussa P-25; Catalyst Loading: 33.33 mg/cm2.
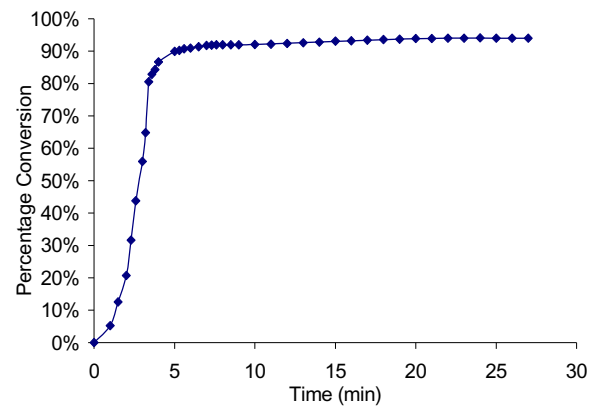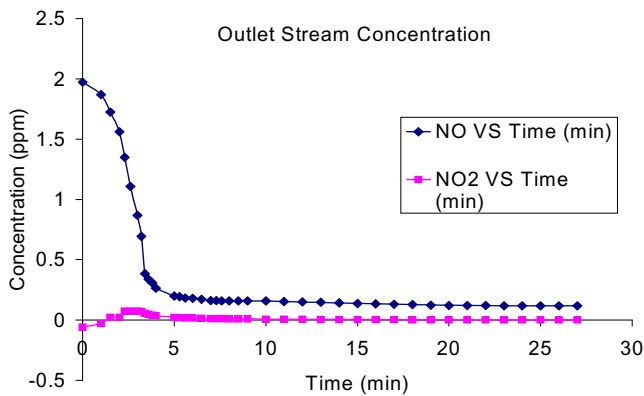

Fig. 2 (a) NO/NO2 concentrations versus time. (b) NO conversion versus time

It can be seen that the NO conversion reached 90% within 5 min. and climbed to stay above that level throughout the experiment. The NO$_2$ level is almost non-detectable except during a transient period within the first 5 minutes, Fig. 2(a)(b). The NO conversion increases from 86-93% with residence time (RT) from 5 - 20 min. Inlet NO concentration has little effect to the steady state NO conversion from 200-2000 ppb. Therefore, the NO conversion is insensitive to the inlet concentration.

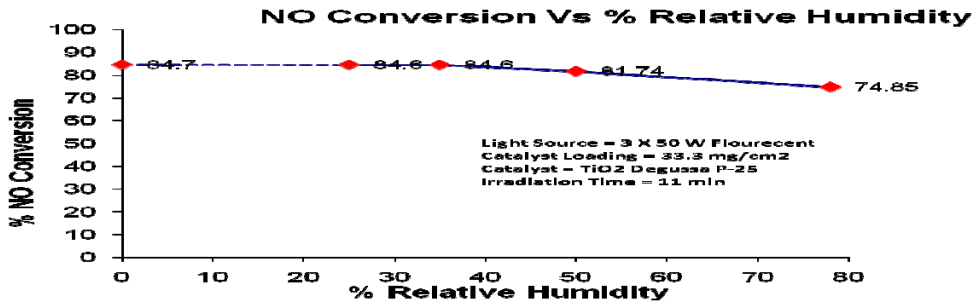Relative Humidity (RH) Effect

Fig. 3 Effect of relative humidity @ Inlet NO Concentration 1000 ppb, RT=5 min

According to the ACI Mix Design Code, the water cement ratio by weight for non-air entrained concrete for 25MPa compressive strength in 28 days is 0.61. Since CCP is already hydroxylated, no need for any excess amount of water even though water is an essential contributor to the OH radical. As shown in Fig. 3, for 1000 ppb inlet NO and 5 min RT, NO conversion is essentially the same for RH = 0-35%; For RH > 35%, NO conversion drops due to the competitive adsorption between water & NO [17].
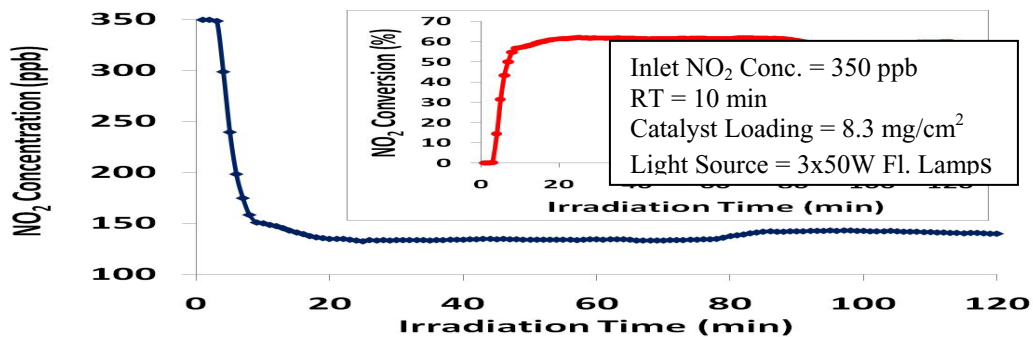

Study of NO_2 Conversion versus Irradiation Time

Figure 4 NO_2 Concentration and Conversion Versus Irradiation Time

Figure 4 shows NO_2 concentration profile vs. irradiation time and the figure embedded shows NO conversion exceeding 60% for an inlet NO_2 concentration of 350 ppb with a residence time of 10 minutes. Thus the NO_2 oxidation is slower as compared to NO oxidation. More work needs to be done for other operating conditions

Ion Chromatograph Test For Nitrite and Nitrate Analysis

After a total of 24 experiments were run, the concrete was washed with deionized water. The liquor was tested for NO_2^- and NO_3^- with a Dionex ICS-1000 Ion Chromatograph (IC). The nitrogen mass balance for the adsorbed species is satisfactory from both the analyzer estimate and the IC results (within 10%). The mass balance of NO, NO_2, NO_2^- and NO_3^- confirms the oxidation of NO to HNO_2 to HNO_3 [12,16].

NO Oxidation Products

When the fluorescent lamp is first turned on, the $\bullet$OH radical quickly reacts with adsorbed NO to form adsorbed HNO_2, as indicated in Figure 5 (a). At this point, the adsorbed HNO_2 can dissociate to H^+ and NO_2^- or react further with $\bullet$OH radical to form adsorbed NO_2 and water. The next reaction in series, *i.e.*, NO_2 reacting with $\bullet$OH radical to form HNO_3, is always fast and eventually reaches equilibrium with its reverse reaction on the surface of the catalyst[12]:
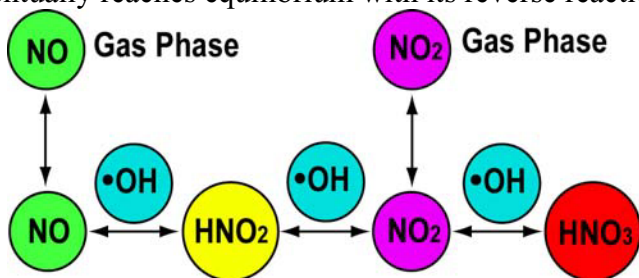

Fig. 5 (a) NO oxidation pathway on catalytic concrete surfaces

Figure 5(b) shows the outlet concentration profile (on a log scale) for an 1000 ppb inlet NO and 5 min and 10 min. RT, which indicates the oxidation of NO to NO_2
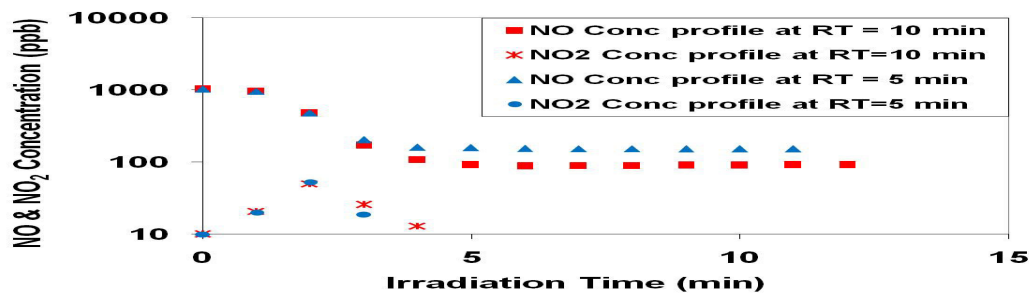

Figure 5(b) NO/NO_2 Concentrations Versus Irradiation Time

[12,18]. The experiment is performed at two different residence times (RT), 5 min and 10 min.

TiO_2 Modified with $BaTiO_3$, Nd_2O_3, and Fe_2O_3 on NO Conversion (Fiber Optic Support)

Figure 6 compares the NO conversion using Degussa P-25 TiO_2 and TiO_2 modified with $BaTiO_3$, Nd_2O_3, and Fe_2O_3. As shown, the steady-state NO conversion for 2 wt% of Fe_2O_3 and 0.15 wt% of Nd_2O_3 (the balance P-25TiO_2) are higher than that of the baseline Degussa P-25 TiO_2. Noticeably NO_2 release to the gas phase is minimal for boosted TiO_2, indicating the enhanced adsorption of NO_2 and oxidation to the final product HNO_3.

**Concentration profile for NO/NO2 using different catalysts**
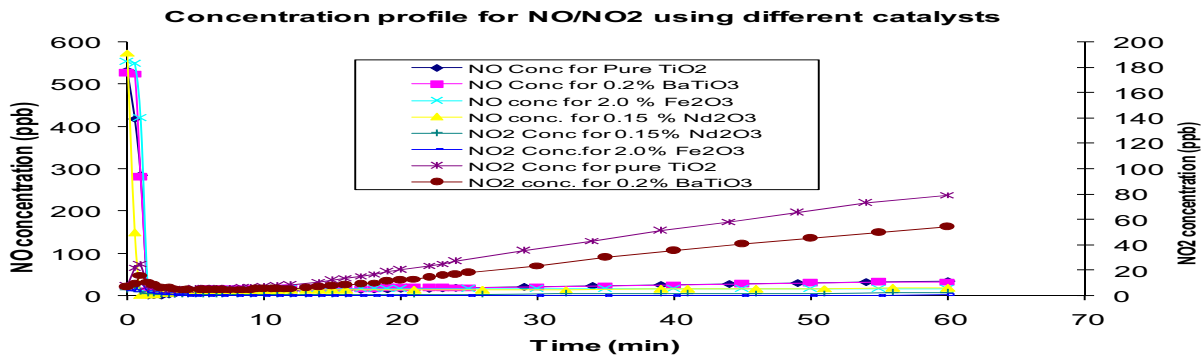
Figure 6 Comparison of NO oxidation for baseline and boosted TiO_2

Concrete Photoreactor with a Uniform Catalytic Layer

Several catalyst-coated concrete photoreactors with small dimensions of 18.5" X 18.5" X 5" were fabricated according to the ACI mix design with a 3-mm catalytic layer with Type 1 Portland cement :Degussa P-25 TiO_2 = 2:1 (weight ratio) and TiO_2 : SiO_2 : CaO : Fe_2O_3 = 1 : 0.58 : 1.77 : 0.09 (mole % ratio). Three 8 watt UVA (Black Light) gives a total radiation exposure is 110 watt/m^2 . The experimental apparatus is essentially the same as in Fig. 7 except more instruments such as ozone analyzer are added. Catalyst loading is 25 mg/m^2 in 3 mm (~1/8") uniform layer. Most experiments were carried out either at 25% relativity humidity (RH) or without adding water vapor (RH=0%). The results indicate that surface coating of TiO_2 is much more effective compared to a uniform layer in terms of NO conversion and NO_2 adsorption. That also suggests a need to investigate different proportions of TiO_2 to cement mixing ratios since a uniform layer is more durable than pure TiO_2 surface coating.

Residence Time Effect (for a uniform layer)

The NO conversion is increasing from 38 – 55% for the residence time 2 – 7 for the inlet NO concentration of 1000 ppb without adding humidity. As the residence time is increasing there is more time for the NO to react photo catalytically. NO_2 yield is defined as $[NO_2]/([NO]_0-[NO])$ where [NO], $[NO_2]$ are NO & NO_2 concentrations, $[NO]_0$ is inlet NO concentration. Both NO_2 concentartion and NO_2 yield decrease with the incresing RT from 2-7 min. Increasing RT allows more time for the oxidation reaction to go to completion (HNO_3).

Steady stae NO & NO2 Cocentration Vs different RT @ Inlet NO CONC of 1000 ppb
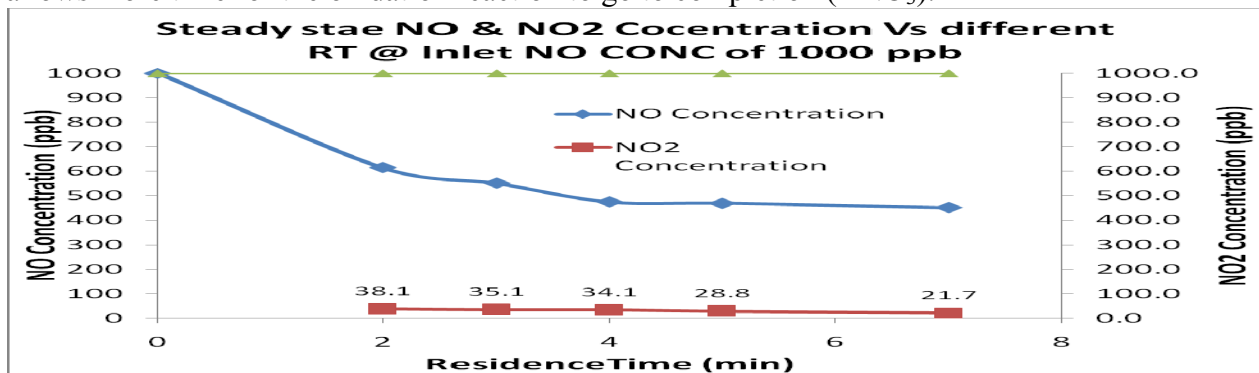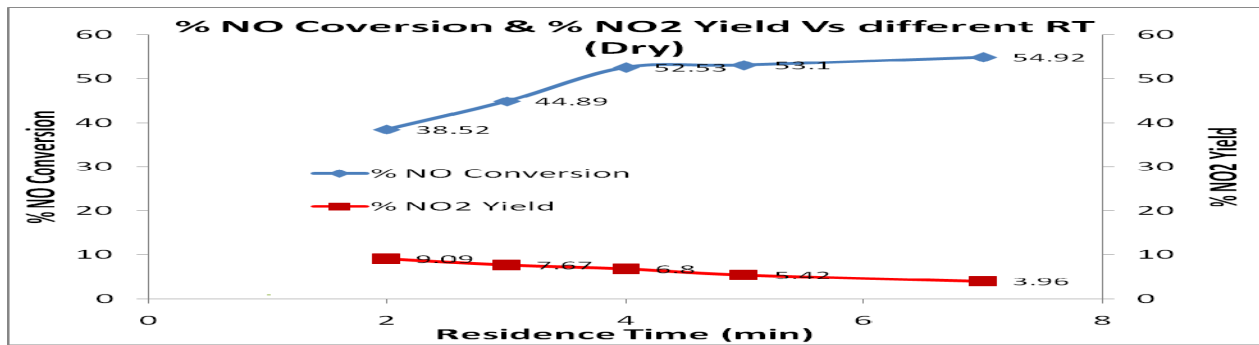
Fig 7: % NO Conversion & NO_2 yield vs Residence Time (without humidity)

Inlet Concentration Effect (for a uniform layer)

The inlet concentration effect were studied @ 5 min Residence time for both dry gases and at 25 % RH. The results are similar. As shown in Fig. 8, the NO conversion decreases from 51 – 28% with increase in inlet NO concentration from 200 – 2000 ppb.
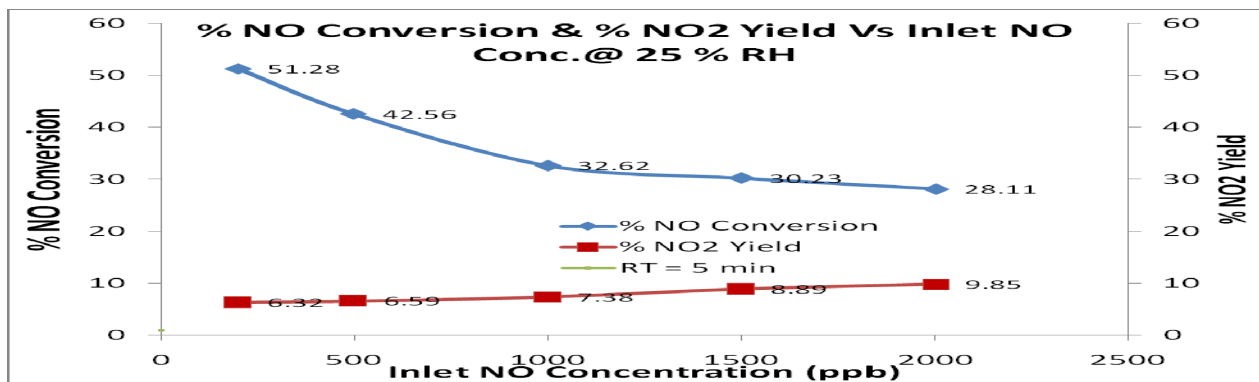

Fig 8: % NO conversion & NO_2 yield vs Inlet NO Concentration for 25% relative humidity

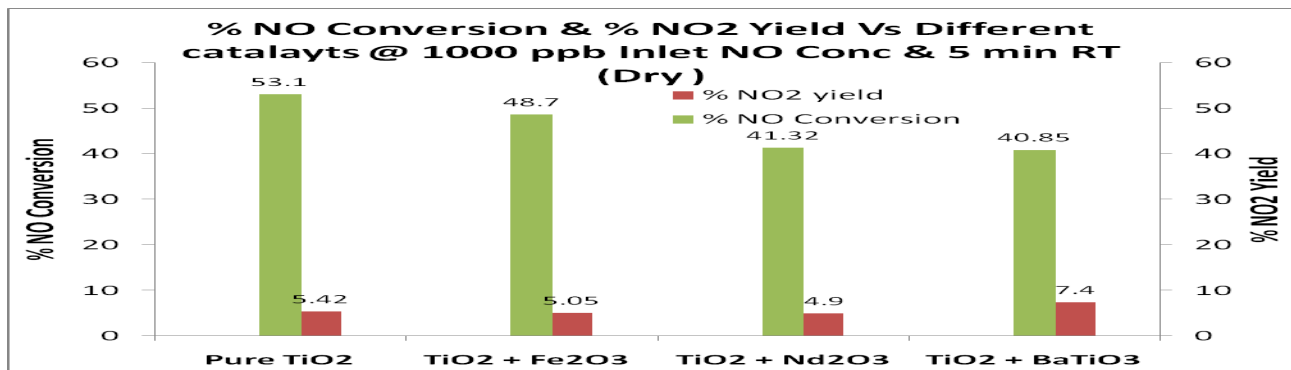NO convesion for different catalyst uniform layers

Fig 9: % NO conversion & NO_2 yield vs different types of catalysts Coated on CCP

Optimize TiO₂: SiO₂: CaO:Fe₂O₃ Ratio

Figure 10 shows twin peaks in the photocatalytic activity of a mixed TiO_2/SiO_2 catalyst synthesized with the sol gel technique. The activity is measured with the oxidation of atrazine, an herbicide, in the aqueous phase under fluorescent light. The interesting phenomena about this result is that pure TiO_2 does not show the highest activity but a certain ratio equivalent to 94% and 16% TiO_2 mole ratio give surprisingly high activity. This together with the fact that Fe_2O_3 enhance NO oxidation at an optimal 2wt% on glass and fiber optic support and Type I Portland cement contains 3.3 mole percent of Fe_2O_3 [19] offer an opportunity to test various proportions of TiO_2 to cement ratio to optimize the ratio of TiO_2: SiO_2:CaO:Fe_2O_3. This may indicate a change of pore structure or surface area in the sol gel catalyst but may also indicate some synergy between TiO_2:SiO_2 and TiO_2:Fe_2O_3 in certain ratios.
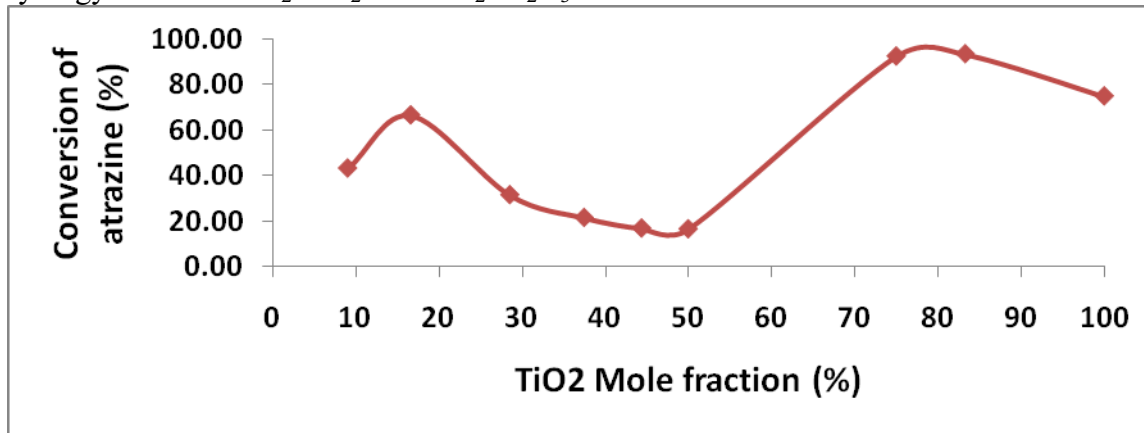
Figure 10 Effect of Mole Fraction of TiO_2 in the TiO_2-SiO_2 Catalyst on Conversion of Atrazine at 60 min Reaction Time

Measurement of O3

Three 15watt UVA lights were used in a 20 L reactor with NO inlet conc.= 1000ppb and RT=5min. No incremental ozone is observed before and after the UVA lamps were turned on or between the inlet and outlet streams during the NO oxidation experiments as shown in Fig. 11. The detection limit is 0.5 ppb. The background O_3 concentrations are between 20-30 ppb.
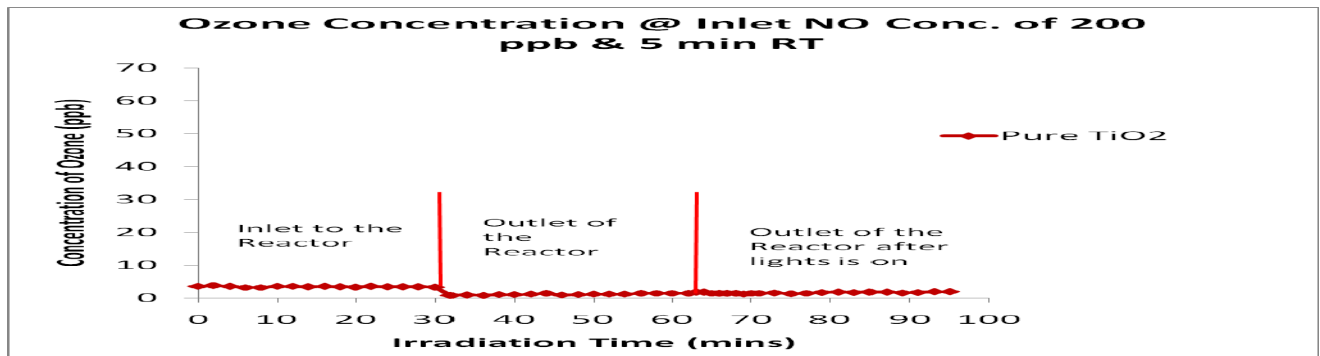
Fig. 11 Ozone measurements @inlet & outlet of the photoreactor coated with P-25 TiO₂

FLUENT Modeling of NOx Plume

In this work, FLUENT 6.3 is used to simulate the NOx dispersion from the exhaust pipe in 3-D. FLUENT follows the finite volume approach to solve the governing transport equations for temperature, pressure, mole fraction and other fluxes [20]. No homogeneous air/NOx reactions or heterogeneous NOx/catalytic surfaces reactions are considered so far but will be included in the third year efforts using the wall surface reactions option in FLUENT. Two conditions have been considered for this study- one is the low-idle condition when the engine runs without the movement of the vehicle for example at a traffic signal or toll-booth and the other is the high-idle condition when the vehicle starts from the stop position. In the low-idle condition, the exhaust exit velocity was taken as 15 m/s and the temperature to be 340 K. In the high-idle condition, the exit velocity was taken as 24m/s and the temperature to be 550K [21]. The composition of the inlet gas was nitric oxide, NO – 350 ppm and nitrogen dioxide, NO_2 – 35 ppm and the background NOx in the atmosphere was NO – 200 ppb, NO_2 – 20 ppb. The concentration of NOx, the temperature and velocity of the plume from the exhaust pipe decrease along the centerline of the plume and along the distance from the exhaust pipe. The concentration of the NOx falls rapidly by the time plume reaches a distance of approximately 3 m downstream from the exhaust pipe, Fig. 12. The turbulence created between the atmosphere and the exhaust plume helps in dispersing the plume. By the time, the plume travels the distance of 10m along the centerline, NOx disperses and it gets to minimum concentration of 200 ppb in the atmosphere.
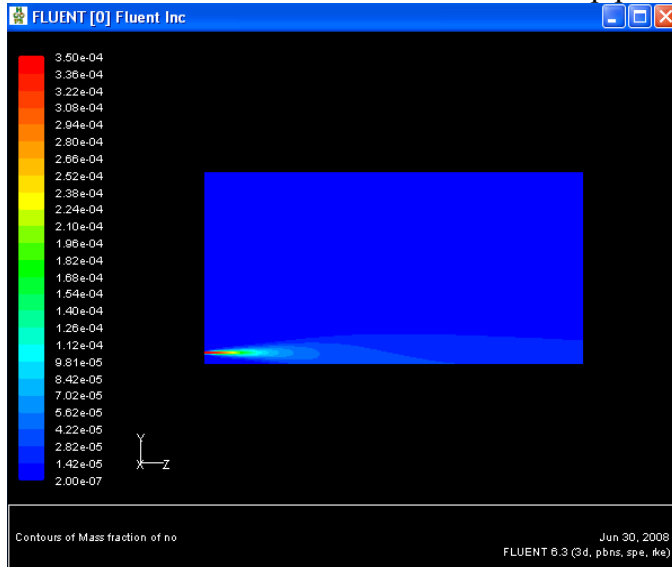
Figure 12 NO Mass Fraction Contours for Low-Idle Condition

References

1. http://www.tceq.state.tx.us/subject/subject_air.html
2. EPA/451-K-97-002, Ozone, October 1997
3. EPA 420-R-99-023, Regulatory Impact Analysis, December 22, 1999, IV-13.
4. http://www.epa.gov/air/urbanair/nox/what.html.
5. http://www.epa.gov/air/urbanair/nox/effrt.html

6. National Renewable Energy Laboratory (2001, October). *Photochemical treatment of pollutants* (CDS-SS25-B001). CO.

7. Fujishima, A., Hashimoto, K. & Wuatanabe, T. (1999). *TiO2 photocatalysis fundamentals and applications* (p. 126 – 156). Tokyo: Bkc, Inc.

8. Frantisek Peterka, Photocatalytic surfaces with self cleaning properties, 6th European Commission Conference on Sustaining Europe's Cultural Heritage: from Research to Policy Queen Elizabeth II Conference Centre, London, UK, 1-3 September 2004.

9. EPA Handbook for Advanced Photochemical Oxidation Process, December 1998, EPA/625/R-981004.

10. Hogan, J. 2004. "Smog-busting paint soaks up noxious gases." *New Scientist*. February 4. http://www.newscientist.com/news/news.jsp?id=ns99994636

11. Takeuchi, K. et al."Removal of nitrogen Oxides from Air by Photocatalysis Using Cement-Immobilized Titanium Dioxide," paper presented in *the Second International Conference on TiO2 Photocatalytic Purification and Treatment of Water and Air*, London, Cincinnati, Ohio, October 26-29, 1996.

12. Sid Devahasdin, Chiun-Jr Fan, Kuyen Li, and Daniel H. Chen, "TiO2 Photocatalytic Oxidation Of Nitric Oxide: Transient Behavior And Reaction Kinetics" *Journal of Photochemistry and Photobiology A; Chemistry,* **156**/1-3 pp 161 – 170 (2003).

13. K. Vajifdar, K. Kotnis, B. Ardoin, D. Chen, K. Li, "Photo catalytic Oxidation of PCE over Titania modified by Non Linear Optical Materials", P132, *TOCAT4*, Tokyo, Japan, July 14-19, 2002.

14. K. Vajifdar, T. Han , B. Ardoin, D. Grooms, D. H. Chen, and K. Li, "Fiber-Optic Photo reactor Using Titania Modified with Ferroelectric Optical Crystals for VOC Destruction", *13th International Congress on Catalysis Conference*, Paris, France, July 11-16, 2004.

15. X. Ye, V. Shah, K. Vajifdar, B. Ardoin, D.H. Chen and K. Li, "VOC oxidation with Various Titania Including Visible-Light-Responsive TiO_2 modified with Ferroelectric Optical $LiNbO_3$," *7th World Congress of Chemical Engineering*, Glasgow, Scotland, July 10-14, 2005.

16. K. Vajifdar, D. Chen, J. Gossage, K. Li, X. Ye, G. Gadiyar and B. Ardoin, "Photocatalytic oxidation of PCE and Butyraldehyde over Titania modified with perovskite optical crystal $BaTiO_3$", *Chemical Engineering and Technology*, 30(4), pp 1-8, 2007.

17. H. Tawara, *et. al.*, "Development of evaluation method of air purifying paving blocks for NOx removal capacity", *Proceedings of The Fourth International conference on TiO_2 Photocatalytic Purification and Treatment of Water and Air*, Albuquerque, NM, 24-28, May 1999.

18. Wang, S. M.E.S. Thesis, Lamar University, Beaumont, TX, 1995.

19. http://original.britannica.com/eb/article-9115999/Table-2-Approximate-Composition-of-Portland-Cement

20. Fluent Users Guide, FLUENT 6.3.26; Fluent Users Center, www.fluentusers.com (accessed 06/30/08)

21. Wang, J.S.; Chan, T.L.; Cheung, C.S.; Leung, C.W.; Hung, W.T. Three-Dimensional Pollutant Concentration Dispersion of a Vehicular Exhaust Plume in the Real Atmosphere. *Atmos. Environ.*, **2006**, 40, 484-497.